

# Journal of Materials Chemistry B

Accepted Manuscript



This is an *Accepted Manuscript*, which has been through the Royal Society of Chemistry peer review process and has been accepted for publication.

*Accepted Manuscripts* are published online shortly after acceptance, before technical editing, formatting and proof reading. Using this free service, authors can make their results available to the community, in citable form, before we publish the edited article. We will replace this *Accepted Manuscript* with the edited and formatted *Advance Article* as soon as it is available.

You can find more information about *Accepted Manuscripts* in the [Information for Authors](#).

Please note that technical editing may introduce minor changes to the text and/or graphics, which may alter content. The journal's standard [Terms & Conditions](#) and the [Ethical guidelines](#) still apply. In no event shall the Royal Society of Chemistry be held responsible for any errors or omissions in this *Accepted Manuscript* or any consequences arising from the use of any information it contains.

## Rational design of a hexapeptide hydrogelator for controlled-release drug delivery

Cite this: DOI: 10.1039/x0xx00000x

Mathieu Bibian,<sup>a</sup> Jeroen Mangelschots,<sup>a</sup> James Gardiner,<sup>b</sup> Lynne Waddington,<sup>b</sup> Maria M. Diaz Acevedo,<sup>c</sup> Bruno G. De Geest,<sup>d</sup> Bruno Van Mele,<sup>c</sup> Annemieke Madder,<sup>e</sup> Richard Hoogenboom<sup>\*,f</sup> and Steven Ballet<sup>\*,a</sup>

Received 00th January 2012,  
Accepted 00th January 2012

DOI: 10.1039/x0xx00000x

www.rsc.org/

The amphiphilic peptide sequence H-Phe-Glu-Phe-Gln-Phe-Lys-OH (MBG-1) is developed as a novel hydrogelator for use in controlled-drug release administration, which is the smallest tunable ionic self-complementary hydrogelating peptide reported to date making it attractive for larger scale preparation. Hydrogelation is demonstrated to result from self-assembly of the peptide into beta-sheet nanofibers that are physically cross-linked by intertwining as well as larger bundle formation. Finally, the release of two small molecule cargos, fluorescein sodium and ciprofloxacin hydro-chloride, is demonstrated revealing a two-stage zero-order sustained release profile up to 80% cumulative release over eight days.

<sup>a</sup>Research Group of Organic Chemistry, Vrije Universiteit Brussel, Pleinlaan 2, Brussels, B-1050, Belgium

<sup>b</sup>Materials Science & Engineering, Commonwealth Scientific and Industrial Organization, Bayview Ave, Clayton, VIC 3169, Australia

<sup>c</sup>Physical Chemistry and Polymer Science, Vrije Universiteit Brussel, Pleinlaan 2, Brussels, B-1050, Belgium

<sup>d</sup>Department of Pharmaceutics, Ghent University, Harelbekestraat 72, Ghent, 9000, Belgium

<sup>e</sup>Organic and Biomimetic Chemistry Research Group, Ghent University, Krijgslaan 281, 9000 Ghent, Belgium

<sup>f</sup>Supramolecular Chemistry Group, Department of Organic Chemistry, Ghent University, Krijgslaan 281, 9000 Ghent, Belgium

† Electronic Supplementary Information (ESI) available. See DOI: 10.1039/b000000x/

### Introduction

Water gelators for the formation of hydrogels have received increasing interest from the scientific community in the last 20 years.<sup>1,2</sup> They have been used as drug delivery systems,<sup>3</sup> cell growth media<sup>4</sup> and many other biomaterial-related applications.<sup>5</sup> Two main types of hydrogels exist: chemical hydrogels, derived from covalently crosslinked polymers, and physical hydrogels based on small molecule hydrogelators that form (fiber) networks by supramolecular interactions. Whereas the chemical hydrogels rely on chemical bonds for their internal structure, physical hydrogels are underpinned by non-covalent interactions such as ionic, hydrophobic and Van der Waals interactions, rendering them reversible and adaptive in nature.<sup>6</sup> Herein, we report the synthesis and characterization of a relatively simple, but tunable, hexapeptide, solely consisting of natural amino acids, able to form a stable hydrogel under physiologically relevant conditions and that exhibits promising release properties for hydrophobic small molecule cargos.

Despite the vast amount of work published on peptide hydrogels in recent years, when aiming for the controlled-delivery of drugs, specific challenges still need to be addressed. These include fine-tuning of mechanical properties, control over drug release rate and mechanism, and the determination of (long-term) toxicity.<sup>7</sup> The use of unprotected and unmodified  $\alpha$ -peptides, i.e. peptides composed of natural  $\alpha$ -amino acids and

lacking any synthetic protecting group, to build hydrogels, can provide advantages over synthetic polymers or non-peptide-based Low Molecular Weight Gelators (LMWGs).<sup>8</sup> One specific advantage is the favorable biocompatibility and biodegradation of such hydrogels as only natural building blocks, L-amino acids, are released upon degradation.

The first reported  $\alpha$ -peptide, EAK16 (Ac-AEAEAKAKAEAEAKAK-NH<sub>2</sub>) (**1**), reported to self-assemble into a  $\beta$ -sheet structure and, ultimately, to form a stable hydrogel in phosphate buffer saline (PBS) solution, was communicated by Zhang et al. (Table 1).<sup>9</sup> This hydrogel was shown to be stable toward proteolysis, temperature and pH changes. Zhang introduced the concept of ‘‘Peptide Lego’’ to classify EAK16 and similar ionic self-complementary peptides.<sup>10</sup> Based on this pioneering work, other groups have reported smaller gel-forming peptides, including the octapeptide H-FEFKFEFK-OH (**2**), being the smallest reported  $\alpha$ -peptide that still allows tuning of amino acid structures to tune the hydrogel properties, to date.<sup>11,12</sup> More recently, Bowerman reported the analogous hydrogel-forming  $\alpha$ -peptide (**3**), (FKFE)<sub>2</sub>, and demonstrated that it also serves as starting point for playing ‘Peptide Lego’, i.e. they observed that many analogues of (**3**) formed fibrillar hydrogels, whereby non-aromatic peptides formed weaker gels than aromatic analogues.<sup>13</sup>

**Table 1** Selected peptide-based hydrogels reported in the literature and their sequences

Compound	Name	Peptide sequence	Ref
1	EAK-16	Ac-AEAEAKAKAEAEAKAK-NH <sub>2</sub>	8
2	FEFKFEFK	H-FEFKFEFK-OH	9
3	(FKFE) <sub>2</sub>	Ac-FKFEFKFE-NH <sub>2</sub>	11
4	<b>MBG-1</b>	H-FEFQFK-OH	<b>This work</b>

In the present study, our aim was to design an even shorter, amphiphatic,  $\alpha$ -peptide hydrogelator that can still be used for 'Peptide Lego' to tune the hydrogel properties as shortening the

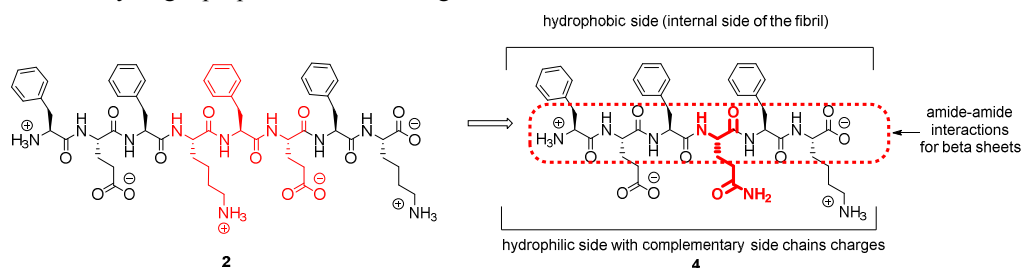


**Fig. 1** Structure of peptides 2 and 4 (MBG-1). The central KFE tripeptide segment in 2 is replaced with Q. The hydrophobic face is involved in  $\pi$ - $\pi$  interactions, the hydrophilic face in charge/H-bonding interactions.

## Experimental procedures

### Peptide synthesis

MBG-1 was synthesized according to standard solid-phase peptide synthesis procedures (see supporting information).<sup>14</sup> Preparative reverse-phase high-performance liquid chromatography (HPLC) was used for purification of the crude peptides. In the purification of MBG-1, solvent A was 0.1% mass fraction TFA in water and solvent B was 0.1% mass fraction TFA in acetonitrile. The chromatographic method of peptide purification was 3-100% B in 0-20 min with a linear gradient. The purity of each peptide was verified by analytical reverse-phase liquid chromatography (RPLC) methods with the same solvent and methods used for preparative RPLC. The resulting pure peptides were obtained after lyophilisation of the collected fractions.

### Preparation of peptide hydrogels

The TFA salt of hexapeptide H-Phe-Glu-Phe-Gln-Phe-Lys-OH (1 or 2 mg) was dissolved in 50  $\mu$ l Milli-Q (mQ) water followed by the addition of 50  $\mu$ l PBS solution. Milli-Q water (with a resistivity of 18.2 m $\Omega$ .cm) refers to ultrapure laboratory grade water that has been filtered and purified by reverse osmosis. This mixture was left to rest overnight, resulting in a 1% or 2% w/v hydrogel, respectively.

sequence by two amino acid residues significantly simplifies the synthesis and purification of larger quantities, as required for hydrogel applications. Even though,  $\alpha$ -peptide hydrogelators with two or three amino acids are known, structural variations immediately lead to loss of hydrogelating ability as it leads to complete solubility or insolubility. Therefore, an  $\alpha$ -peptide of intermediate length, a hexamer, was designed with structural analogy to octapeptide (2). In our designed structure the three central amino acids of octapeptide (2) (K4, F5 and E6) were replaced by a single residue, a glutamine moiety Q, to give hexapeptide (4) referred to as MBG-1 (Fig. 1). The amide group of the glutamine side chain can be considered both as a H-bond acceptor and donor. This, combined with the more hydrophobic nature of a primary amide function (compared to an ammonium or a carboxylate group of Lys and Glu side chains at physiological pH, respectively), was envisioned to lead to the formation of self-assembled hydrogels.

### Preparation of fluorescein sodium and ciprofloxacin hydrochloride-loaded hydrogels

Fluorescein sodium and ciprofloxacin hydrochloride were dissolved in mQ water (2 mg/ml or 4 mg/ml to obtain a final loading of 0.1% w/v or 0.2% w/v, respectively). The resulting solution was then used following the procedure as described above to obtain a FL or CIP-loaded hydrogel.

### FT-IR analysis

FT-IR spectra were collected on a Nicolet 6700 FT-IR spectrometer in attenuated total reflectance (ATR) mode with diamond ATR sample holder. An aliquot of the gel was transferred on the diamond. Scans were between 4000 and 600  $\text{cm}^{-1}$  with 64 accumulations at a resolution of 0.4  $\text{cm}^{-1}$ .

### Dynamic Rheometry

Dynamic rheometry measurements were carried out on a TA Instruments AR-G2 rheometer equipped with Electrically Heated Plates and aluminum plate-plate geometry with a diameter of 10mm. A ring shaped reservoir filled with a saturated NH<sub>4</sub>Cl solution was placed around the measuring plates for humidity control. Rheological properties of the hydrogels were studied by oscillatory frequency sweeps performed at 30  $^{\circ}\text{C}$  and 37  $^{\circ}\text{C}$  in the range between 0.01 and 10 Hz using a strain control of 0.05%.

### CD analysis

The secondary structure of the peptides was analyzed using a 0.1 cm quartz cell on a Jasco J815 Spectropolarimeter, with 1 s integrations, 1 accumulation and a step size of 1 nm with a band width of 1 nm over a range of wavelengths from 200 to 270 nm. Peptide samples were freshly prepared directly in the CD cell, and spectra were recorded after 2h. Measurements were repeated at least 3 times and their average was plotted.

### Release studies

Self-assembled peptide hydrogels with a loading of 0.1% w/v or 0.2% w/v were directly prepared in a 1.5 ml eppendorf, following the procedure as described above (with final gel volume of 0.1 ml). Without disrupting the hydrogel, 0.5 ml of PBS buffer (pH = 7.4) was gently added on top of the hydrogel. At selected time points 10  $\mu$ l of the supernatant PBS solution was taken and replaced with 10  $\mu$ l of fresh PBS buffer. Samples were analyzed by HPLC and the absorbance was monitored over time. The percent fraction of release was obtained by integrating the absorbance signals of the HPLC spectra (FL at 215 nm and CIP-HCl at 273 nm). The release profiles, expressed as recovery curves, were obtained by plotting the percent fraction as a function of time. Each experiment was repeated in triplicate, and mean and standard error were calculated in Excel.

### Cryo-TEM analysis

A laboratory-built humidity-controlled vitrification system was used to prepare the hydrogels for imaging in a thin layer of vitrified ice using cryo-TEM. Humidity was kept close to 80% for all experiments, and ambient temperature was 22°C. 200 Mesh copper grids coated with perforated carbon film (Lacey carbon film: ProSci- Tech, Qld, Australia) were used for all experiments. Grids were glow discharged in nitrogen for 5 s immediately before use. Hydrogels were prepared as described above and analysed after 24 h. Approximately 4  $\mu$ L aliquots of sample were pipetted onto each grid prior to plunging. After 30 s adsorption time the grid was blotted manually using Whatman 541 filter paper. The grid was then plunged into liquid ethane cooled by liquid nitrogen. Frozen grids were stored in liquid nitrogen until required. The samples were examined using a Gatan 626 cryoholder (Gatan, Pleasanton, CA, USA) and Tecnai 12 Transmission Electron Microscope (FEI, Eindhoven, The Netherlands) at an operating voltage of 120 kV. At all times low dose procedures were followed, using an electron dose of 8-10 electrons  $\text{\AA}^{-2}$  for all imaging. Images were recorded using an FEI Eagle 4kx4k CCD camera (FEI, Eindhoven, The Netherlands).

### Negative staining TEM analysis

Carbon-coated 300-mesh copper grids were glow-discharged in nitrogen to render the carbon film hydrophilic. Hydrogels were prepared as described above, diluted to allow handling, and a 4  $\mu$ l aliquot of the sample was pipetted onto each grid. After 30

seconds adsorption time, the excess was drawn off using Whatman 541 filter paper, followed by staining with 2% aqueous potassium phosphotungstate at pH 7.2, for 10 s. Grids were air-dried until needed. The samples were examined using a Tecnai 12 Transmission Electron Microscope (FEI, Eindhoven, The Netherlands) at an operating voltage of 120KV. Images were recorded using a Megaview III CCD camera and AnalySIS camera control software (Olympus.) Each grid was systematically examined and imaged to reflect a representative view of the sample.

## Results and discussion

The physicochemical conditions inducing gelation of MBG-1 were studied, revealing that this peptide was completely soluble in mQ water, even at a 1% w/v concentration. However, the addition of PBS yielding a volume ratio of 1:1 water/PBS resulted in the formation of a strong hydrogel. The ions in the PBS solution are known to induce a salting out effect, proposedly leading to enhanced hydrophobic association and the formation of peptide nanofibers that cause the solution to gel.<sup>15</sup> This was confirmed by successful hydrogelation of a solution of MBG-1 (1 wt%) in mQ water upon addition of 100  $\mu$ L of a 150 mM NaCl solution, thereby ruling out that ionic crosslinking by multivalent phosphate anions is the driving force for hydrogelation. The salt-induced hydrogelation behavior of MBG-1 has important consequences as it allows subcutaneous injection of a liquid aqueous solution of MBG-1 in mQ, resulting in in situ gel-formation due to an increase in ionic strength in vivo. As such, MBG-1 is the shortest reported peptide sequence that acts as an ionic self-complementary hydrogelator for the 'Peptide Lego' concept.

The mechanical properties of this MBG-1 hydrogel in water/PBS were studied using dynamic rheometry at both 30°C and 37°C (Fig. 2), whereby the viscoelastic properties of a hydrogel are defined by the storage modulus ( $G'$ , corresponding to elastic deformation), the loss modulus ( $G''$ , corresponding to viscous flow) and the loss factor ( $\tan\delta$ , defined as the  $G''/G'$  ratio). Rheology of the MBG-1 hydrogel in water/PBS, both at 30°C and 37°C, revealed a frequency-independent loss angle of ca. 10°, demonstrating the formation of a solid-like hydrogel.<sup>16</sup> The storage modulus,  $G'$ , of ca. 10 kPa at 37°C is indicative for a rather rigid hydrogel, and under identical conditions, MBG-1 showed a higher rigidity ( $G'$ ) than a reference hydrogel of octapeptide (2) (see supporting information). Although an increase of the temperature from 30°C to 37°C led to slightly higher  $G'$  and  $G''$  values (Fig. 2), the  $\tan\delta$  or phase angle  $\delta$  nearly remained constant, which indicates that this temperature change does not significantly influence the nature of the hydrogel. The slight increase in  $G'$  with increasing temperature indicates that the self-assembly is mainly entropy driven, i.e. it is driven by the release of bound water molecules.<sup>17</sup> The combination of the PBS induced hydrogelation and the favorable rheological properties under such physiologically relevant conditions, render MBG-1 a strong lead peptide for biomaterial applications, whereby it is speculated that its exact



structure may be further tailored to optimize the hydrogel properties for specific applications via the 'Peptide Lego' concept.

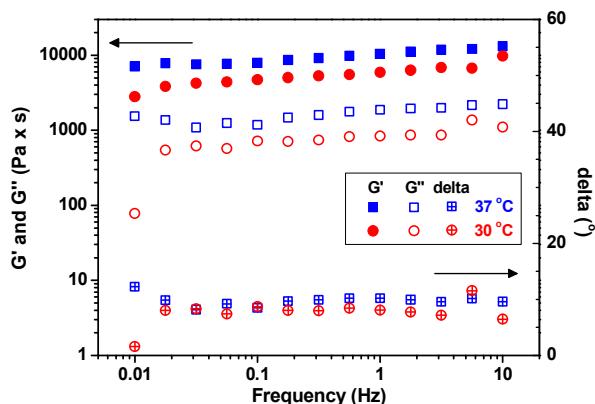


**Fig. 2** Rheological analysis of MBG-1 (1% w/v) in 1:1 PBS/water at 30°C and 37°C.

In order to further understand the hydrogelation mechanism of MBG-1, cryo-transmission electron microscopy (CryoTEM) and negative staining TEM were used to analyze the morphology of the hydrogel (1:1 PBS/water), revealing the presence of very long slender fibrils (5-8 nm width), mostly straight or gently curved, with very distinctive periodicity resembling the classic amyloid morphology (Fig. 3A). In some cases fibers are intertwined to form extended supercoiled helical structures (see arrows Fig. 3B) with a period of approximately 100 nm. Larger, thicker structures were also observed (20-30 nm) that appear tubular in nature (Fig. 3C) Negative staining (to increase local contrast) confirmed the morphology of these larger tubular structures and suggests they result from further assembly of the smaller fibers (Fig 3D-F).

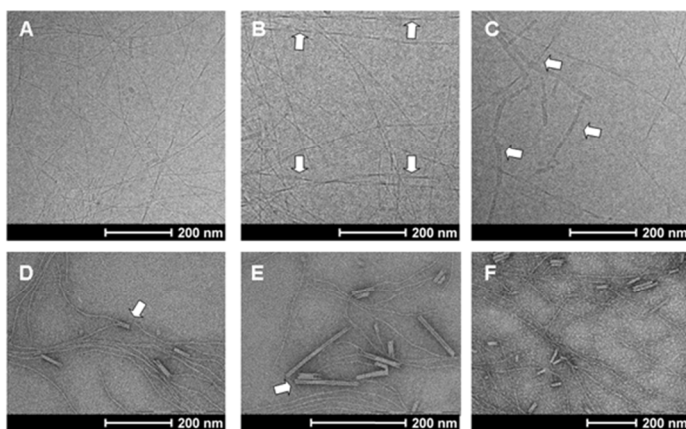
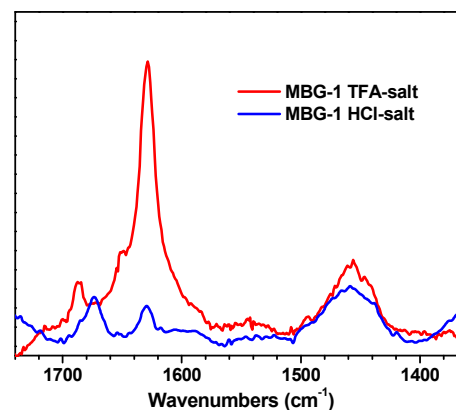


**Fig. 3** CryoTEM (A-C) and negative staining TEM (D-F) analysis of MBG-1 displaying fiber polymorphism. In figures B, C, D and E the white arrows indicate the presence of helical structures or larger tubular structures resulting from an interaction between two or more fibers.

Based on this detailed TEM analysis it is suggested that both the intertwined bundles and tubular structures act as physical crosslinks of individual peptide nanofibers to form a rigid hydrogel.<sup>18</sup>

The self-assembly of MBG-1 was further investigated at the molecular level by FT-IR<sup>19,20</sup> and Circular Dichroism (CD) spectroscopy. In CD spectra classical  $\beta$ -sheets are usually associated with a maximum around 200 nm and a minimum between 214 and 217 nm.<sup>[21]</sup> A maximum around 205 nm and a minimum at 231 nm were observed in the CD spectrum of MBG-1 (See Figure S4 in supporting information). Although this CD spectrum slightly differs from that for classical  $\beta$ -sheets, these characteristics are in line with a previous report of Lee and coworkers on peptide hydrogels.<sup>[22]</sup> Figure 4 depicts the FT-IR analysis of MBG-1 in D<sub>2</sub>O/PBS (PBS solution prepared in D<sub>2</sub>O) (1:1, 1% w/v) and the observed signal frequencies of the amide I bands are in agreement with  $\beta$ -sheet formation (amide I 1629 cm<sup>-1</sup> and 1687 cm<sup>-1</sup>).<sup>19,20</sup> The second intense band at 1674 cm<sup>-1</sup> is the characteristic absorption band for trifluoroacetate (TFA) salt,<sup>23</sup> although it is sometimes erroneously associated with antiparallel  $\beta$ -sheet structure.<sup>19,24,25</sup> In our case, when the trifluoroacetate anion was exchanged for a chloride ion, the band at 1674 cm<sup>-1</sup> disappeared (Fig. 4, red curve), indicating that this band is indeed associated with TFA



salts and not with MBG-1 intermolecular interactions.

**Fig. 4** FT-IR analysis of MBG-1 hydrogels (1% w/v) in D<sub>2</sub>O/PBS 1:1 v/v, PBS solution prepared in D<sub>2</sub>O), whereby MBG-1 was used as TFA salt or HCl salt.

In order to gain further insight into the hydrogel structure and, in particular, the mesh size, fluorescence recovery after photobleaching (FRAP) measurements were attempted with the MBG-1 hydrogel. However, after loading the hydrogel with dextran-fluorescein isothiocyanate (FITC), fluorescence microscopy revealed a very inhomogeneous fluorescence distribution throughout the sample, obstructing the FRAP measurements (see figure supporting info). The inhomogeneous fluorescence distribution, however, indicated specific interactions between dextran-FITC and the gel fibers motivating us to evaluate our hydrogels for the sustained release of small molecules.

It has been previously reported that peptide hydrogels can possess high drug loading capacities in comparison to conventional drug delivery polymer hydrogels (e.g. 1 and 2 mg/ml of drug cargo with 10 mg/ml of peptide gelator, i.e. 10 and 20 weight% resp.).<sup>26,27</sup> Herein, the release properties of the MBG-1 hydrogel were examined for two cargoes. Fluorescein sodium (FL), a planar aromatic molecule (Fig. 5A), was chosen as a model substrate for drug delivery of small molecules from polymer and peptide hydrogels, inspired by the interactions of dextran-FITC with our peptide hydrogel.<sup>28,29</sup> In addition, ciprofloxacin (CIP), one of the most efficient fluoroquinolone antibiotics, was chosen as a clinically more relevant second cargo to compare the release profiles of two small molecules with distinct structural properties (Fig. 5B).

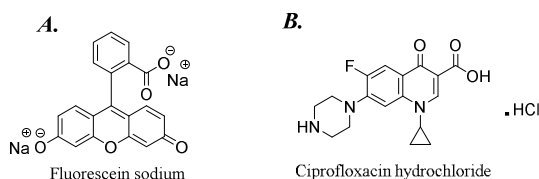


**Fig. 5** Structures of the two investigated cargoes, fluorescein sodium (A) and ciprofloxacin hydrochloride (CIP-HCl) (B), used to assess the release properties of hydrogel MBG-1.

Self-assembled peptide hydrogels with drug loading of 0.1% w/v (fluorescein and CIP-HCl) or 0.2% w/v (CIP-HCl) were directly prepared in a 1.5 ml eppendorf, following the procedure as described in experimental section resulting in a final gel volume of 0.1 ml. Without disrupting the hydrogel, 0.5 ml of PBS buffer (pH = 7.4) was gently added on top of the hydrogel. At selected time points 10  $\mu$ l of the supernatant PBS solution was taken for analysis and replaced with 10  $\mu$ l of fresh PBS buffer.

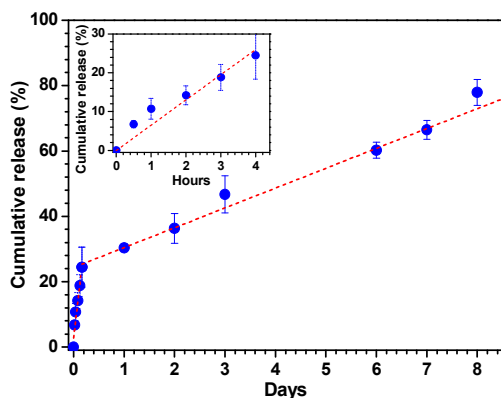


**Fig. 6** Static release experiment of fluorescein sodium (0.1% w/v) from MBG-1 hydrogel (1% w/v in H<sub>2</sub>O/PBS 1:1 v/v) expressed as cumulative release fraction over 8 days and enlargement of the first four hours (inset). Data points represent the average of 3 samples with calculated standard error values; linear fits are added for the first four hours and the remainder of the time to guide the eye.

Initial studies were performed with sodium fluorescein as a cargo (0.1 % w/v concentration) to gain a first insight into the release properties of the MBG-1-based hydrogel (Fig. 6; for a discussion on the reliability of such experiments we refer to the work of Brandl et al.).<sup>30</sup> The initial fast release of a significant proportion of the cargo, also referred to as the burst effect, has often been reported for drug release from small molecule hydrogels.<sup>31</sup>

However, according to Fig. 6, only a moderate burst effect (25% ( $\pm$ 5%) release in 4 hours) was observed during this static experiment with the MBG-1 hydrogel. The release of the fluorescein dye in the first 4 hours (25 %, Fig. 6, inset) is relatively steep in comparison to the slower progressive release over the subsequent days, which, importantly, follows a zero-order release profile (linear increase of cumulative release, Fig. 6). A plateau value of 76% ( $\pm$ 3%) released fluorescein was obtained after 8 days as longer times led to gel collapse into a white opaque structure.

The minor burst release in the first four hours is most likely caused by i) fluorescein molecules that were at or near the PBS-hydrogel interface and escaped rapidly into the PBS solution, ii) rapid cargo release through large pores of the hydrogel, compared with release through local areas consisting of smaller pores due to higher entanglement of the fiber network and/or iii) rapid release of weakly associated fluorescein molecules. Subsequent, zero-order slow release is most likely related to a gradual increase in salt concentration, arising from the supernatant PBS solution, as the peptide is not soluble in pure PBS. This collapse of the hydrogel is proposedly driven by slow dehydration and hydrophobic aggregation of, presumably, bundles of peptide fibers leading to simultaneous release of the entrapped cargo, as the hydrophobic peptide surface area, where the cargo is expected to be adsorbed, decreases.<sup>3</sup> This proposed hydrophobic drug delivery mechanism, by breaking apolar interactions with the phenylalanine side chains releases the drug, may be rationalized by the hydrophobic/aromatic nature of fluorescein.<sup>31</sup> This proposed hydrophobically induced drug release mechanism is supported by the minor burst effect, the relatively slow rate of release, and the appearance of aggregation (evidenced by opacity of the hydrogel which occurred after approximately 5 days release) at the PBS-hydrogel interface and, finally, the full collapse of the hydrogel after 8 days.

Besides fluorescein, ciprofloxacin (CIP) was also used as a cargo to study drug delivery from the MBG-1 hydrogels. Ciprofloxacin is a broad spectrum fluoroquinolone antibiotic in clinical use with approximately 20 million prescriptions written in the US alone in 2010.<sup>32</sup> Although both fluorescein and CIP have similar molar mass (CIP-HCl 367 g/mol vs. FL 376 g/mol), they have very different physicochemical properties (solubility, hydrophobicity, net charge, conformational freedom, etc). While fluorescein is readily soluble in water, the solubility of CIP (0.07 mg/ml at 20°C) in water at physiological

pH is comparatively low and to allow using it as a cargo, we prepared its hydrochloride salt (CIP-HCl) by dissolving the required amount of CIP in 0.4 M HCl solution. The release of CIP-HCl from MBG-1 hydrogels was studied with a 1% w/v MBG-1 hydrogel, loaded with 0.1 % w/v and 0.2% w/v CIP-HCl. The release profiles of CIP-HCl from these hydrogels is remarkably similar demonstrating that the absolute amount of released CIP-HCl can be tuned by the initial cargo loading, i.e. 50  $\mu$ g CIP-HCl release from the 0.1% loaded hydrogel and 100  $\mu$ g from the 0.2% loaded hydrogel (Fig. 7). Similar to the release of fluorescein, the release profile consists of two distinct regimes, starting with a faster linear release for the first two days (40% drug release) followed by very slow sustained release up to 8 days up to maximal cumulative release of 50%.

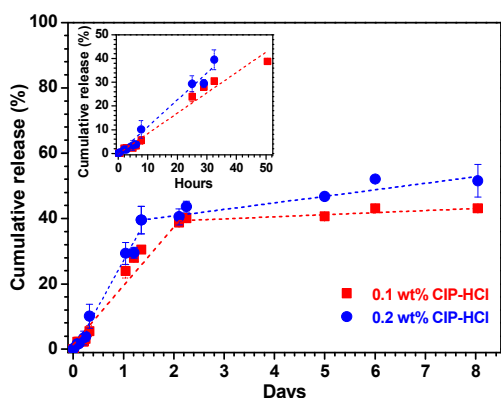


**Fig. 7** Static release experiments of ciprofloxacin hydrochloride (0.1% and 0.2% w/v) from MBG-1 hydrogels (1% w/v in H<sub>2</sub>O/PBS 1:1 v/v) expressed as cumulative release fraction over 8 days and enlargement of the first two days (inset). Data points represent the average of 3 samples with calculated standard error values; linear fits are added for the first four hours and the remainder of the time to guide the eye.

In comparison to fluorescein, the release of CIP-HCl is significantly slower, in agreement with the proposed hydrophobic drug encapsulation mechanism, as CIP-HCl is more hydrophobic than fluorescein and will be more strongly associated to the MBG-1 hydrogel fibers. This stronger association is also responsible for the lower total cumulative release of CIP-HCl compared to fluorescein. It is important to note that the release profiles of CIP-HCl from the 1% w/v MBG-1 hydrogel shows a significantly more sustained release compared to the single other reported study on the release of CIP from a peptide hydrogel, based on a (D-Leu-Phe-Phe-OH) tripeptide, demonstrating a burst release of 45% of the loaded CIP within the first 10 hours followed by a plateau and a maximum release of approximately 50% after 6 days.<sup>26</sup> In contrast, CIP-HCl release from MBG-1 resulted in 40% release over the first 30-50h (depending on loading, Fig. 7) followed by a plateau and gradual release towards the maximum of 50% over 8 days. As such, the MBG-1 hydrogel results in much more sustained release, which is much more desirable when

considering therapeutic applications of hydrogels for drug delivery.

## Conclusions

In summary, we have developed a novel hexapeptide hydrogelator, MBG-1, able to induce gelation in a mixture of water and PBS, proposedly facilitating injection induced in vivo gelation. This hexapeptide is the shortest sequence known that forms an amphipathic self-assembling structure, which makes it highly interesting for the 'Peptide Lego' concept. Besides an economical advantage of a shortened sequence, the rheological properties suggest it to be an interesting candidate for drug delivery technology as a rigid gel was obtained.

CryoTEM and negative staining TEM revealed that the hydrogelation of MBG-1 is driven by its self-assembly into long thin fibers that are physically crosslinked by the formation of higher order intertwined and tubular structures. At a molecular level, FTIR and CD analysis (see supporting information) indicated the presence of  $\beta$ -sheets as the predominant structure underlying the self-assembly of MBG-1 into nanofibers. Furthermore, we have demonstrated that MBG-1 hydrogels revealed favorable release profiles for fluorescein and ciprofloxacin with controlled and sustained in vitro release profiles spanning up to 8 days.

The great diversity of available natural amino acids will allow us to easily access modified analogues of MBG-1 to further tune the gel formation conditions, hydrogel properties and release profiles. As such, the reported hexapeptide MBG-1 opens up new avenues for peptide hydrogels, both from a fundamental view as well as for applications.

## Acknowledgements

We thank the Research Foundation - Flanders (FWO Vlaanderen) for the financial support.

Mathieu Bibian and Jeroen Mangelschots contributed equally to this work.

## References

- 1 C. J. Bowerman and B. L. Nilsson, *Biopolymers*, 2012, **98**, 169.
- 2 C. Tomasini and N. Castellucci, *Chem. Soc. Rev.*, 2013, **42**, 156.
- 3 T. R. Hoare and D. S. Kohane, *Polymer*, 2008, **49**, 1993.
- 4 A. Mujeeb, A. F. Miller, A. Saiani and J. E. Gough, *Acta Biomater.*, 2013, **9**, 4609.
- 5 J. L. Drury and D. J. Mooney, *Biomaterials*, 2003, **24**, 4337.
- 6 J. Kopecek and J. Yang, *Acta Biomater.*, 2009, **5**, 805.
- 7 Y. Kuang and B. Xu, *Angew. Chem. Int. Ed. Engl.*, 2013, **1**.
- 8 N. Castellucci, G. Sartor, N. Calonghi, C. Parolin, G. Falini and C. A. Tomasini, *Beilstein J. Org. Chem.*, 2013, **9**, 417.
- 9 S. Zhang, T. Holmes and C. Lockshin, *A. Rich, Proc. Natl. Acad. Sci. U. S. A.*, 1993, **90**, 3334.
- 10 S. Zhang, *Nat. Biotechnol.*, 2003, **21**, 1178.
- 11 A. Mohammed, A. F. Miller and A. Saiani, *Macromol. Symp.*, 2007, **251**, 88.

- 12 M. R. Caplan, P. N. Moore, S. Zhang, R. D. Kamm and D. A. Lauffenburger, *Biomacromolecules*, 2000, **1**, 627.
- 13 C. J. Bowerman, D. M. Ryan, D. A. Nissan and B. L. Nilsson, *Mol. Biosyst.*, 2009, **5**, 1058.
- 14 W. C. Chan and P. D. White, *Fmoc Solid Phase Peptide Synthesis: A Practical Approach*, Oxford University Press, New York 2000.
- 15 P. J. Marek, V. Patsalo, D. F. Green and D. P. Raleigh, *Biochemistry*, 2012, **51**, 8478.
- 16 C. Yan and D. J. Pochan, *Chem. Soc. Rev.*, 2010, **39**, 3528.
- 17 V. J. Nebot, J. Armengol, J. Smets and S. F. Prieto, *Chem. Eur. J.*, 2012, **18**, 4063.
- 18 P. H. J. Kouwer, M. Koepf, V. A. A. Le Sage, M. Jaspers, M. A. Van Buul, Z. H. Eksteen-Akeroyd, T. Woltinge, E. Schwartz, H. J. Kitto, R. Hoogenboom, S. J. Picken, R. J. M. Nolte, E. Mendes and A. E. Rowan, *Nature*, 2013, **493**, 651.
- 19 A. Barth and C. Zscherp, *Q. Rev. Biophys.*, 2002, **35**, 369.
- 20 J. Kong and S. Yu, *Acta Biochim. Biophys. Sin. (Shanghai)*, 2007, **39**, 549.
- 21 S. M. Kelly, N. C. Rice, *Curr. Protein Pept. Sci.* 2000, **1**, 349.
- 22 N. R. Lee, C. J. Bowerman, B. L. Nilsson, *Biomacromolecules* 2013, **14**, 3267.
- 23 C. J. Bowerman, W. Liyanage, A. J. Federation and B. L. Nilsson, *Biomacromolecules*, 2011, **12**, 2735.
- 24 J. Naskar, G. Palui and A. Banerjee, *J. Phys. Chem. B.*, 2009, **113**, 11787.
- 25 Y. Mazor, S. Gilead, I. Benhar and E. Gazit, *J. Mol. Biol.*, 2002, **322**, 1013.
- 26 J. Ruiz, A. Mantecón and V. Cádiz, *J. Appl. Polym. Sci.*, 2001, **85**, 1644.
- 27 S. Marchesan, Y. Qu, J. Waddington, C. D. Easton, V. Glattauer, T. J. Lithgow, K. M. McLean, J. S. Forsythe and P. G. Hartley, *Biomaterials*, 2013, **34**, 3678.
- 28 T. J. Dursch, N. O. Taylor, D. E. Liu, R. Y. Wu, J. M. Prausnitz and C. J. Radke, *Biomaterials*, 2014, **35**, 620.
- 29 R. Censi, P. D. Martino, T. Vermonden and W. E. Hennik, *J. Control. Release*, 2012, **161**, 680.
- 30 F. Brandl, F. Kastner, R. M. Gschwind, T. Blunk, J. Tessmar and A. Göpferich, *J. Control. Release*, 2010, **142**, 221.
- 31 T. Vermonden, R. Censi and W. E. Hennink, *Chem. Rev.*, 2012, **112**, 2853.
- 32 B. J. Knotterus, L. Grigoryan and S. E. Geerlings, *Fam. Pract.*, 2012, **29**, 659.